

SEARCHING FOR OVERTURNING CONVECTION IN PENUMBRAL FILAMENTS: SLIT SPECTROSCOPY AT 0.2 ARCSEC RESOLUTION

L.R. BELLOT RUBIO¹, R. SCHLICHENMAIER², AND K. LANGHANS³

¹Instituto de Astrofísica de Andalucía (CSIC), Apdo. 3004, 18080 Granada, Spain

²Kiepenheuer-Institut für Sonnenphysik, Schöneckstr. 6, 79104, Freiburg, Germany, and

³Sickingenweg 10, 23568 Lübeck, Germany

To appear in ApJ. Accepted 2010 September 24

ABSTRACT

Recent numerical simulations of sunspots suggest that overturning convection is responsible for the existence of penumbral filaments and the Evershed flow, but there is little observational evidence of this process. Here we carry out a spectroscopic search for small-scale convective motions in the penumbra of a sunspot located 5° away from the disk center. The position of the spot is very favorable for the detection of overturning downflows at the edges of penumbral filaments. Our analysis is based on measurements of the Fe I 709.0 nm line taken with the Littrow spectrograph of the Swedish 1 m Solar Telescope under excellent seeing conditions. We compute line bisectors at different intensity levels and derive Doppler velocities from them. The velocities are calibrated using a nearby telluric line, with systematic errors smaller than 150 m s⁻¹. Deep in the photosphere, as sampled by the bisectors at the 80%-88% intensity levels, we always observe blueshifts or zero velocities. The maximum blueshifts reach 1.2 km s⁻¹ and tend to be cospatial with bright penumbral filaments. In the line core we detect blueshifts for the most part, with small velocities not exceeding 300 m s⁻¹. Redshifts also occur, but at the level of 100-150 m s⁻¹, and only occasionally. The fact that they are visible in high layers casts doubts on their convective origin. Overall, we do not find indications of downflows that could be associated with overturning convection at our detection limit of 150 m s⁻¹. Either no downflows exist, or we have been unable to observe them because they occur beneath $\tau = 1$ or the spatial resolution/height resolution of the measurements is still insufficient.

Subject headings: convection – sunspots – Sun: photosphere – Sun: surface magnetism

1. INTRODUCTION

The origin of the Evershed flow is not completely understood (Borrero 2009; Scharmer 2009; Schlichenmaier 2009; Bellot Rubio 2010; Nordlund & Scharmer 2010). Models based on moving flux tubes explain the flow in terms of a pressure gradient that builds up along the tubes as they rise from the sunspot magnetopause (Schlichenmaier et al. 1998; Schlichenmaier 2002), whereas siphon flow models invoke pressure gradients created by different field strengths at the footpoints of elevated magnetic arches (e.g., Meyer & Schmidt 1968; Degenhardt 1989; Montesinos & Thomas 1997). In both cases, mass conservation is secured by downflows that occur in the mid and outer penumbra as the field lines return to the solar surface.

Another possibility is that the Evershed flow is caused by convection in the presence of the sunspot magnetic field, which induces an anisotropy in the radial direction. The idea was put forward by Scharmer et al. (2008) and seems to be supported by radiative magnetohydrodynamic simulations (Heinemann et al. 2007; Rempel et al. 2009a,b). According to the simulations, hot weakly magnetized material ascends in the penumbra and becomes nearly horizontal after being deflected outward by the inclined sunspot field. This results in a penumbral filament —an elongated overturning flow pattern with an upward component at the center (the Evershed flow) and lateral downflows at the edges. The process is similar to granular convection in the quiet Sun, except for the existence of a preferred horizontal direction.

In the simulations one observes narrow (0.''2–0.''4) lanes of downflows on either side of the filaments. They appear where

the Evershed flow returns back to the solar surface. The downflows ensure mass conservation and reach velocities of up to 1.5 km s⁻¹ at optical depth $\tau = 0.1$ (Heinemann et al. 2007; Rempel et al. 2009a). Interestingly, they have a small horizontal component toward the umbra, i.e., their direction is opposite to that of the Evershed flow.

A clear detection of downward motions at the edges of penumbral filaments would support the existence of overturning convection in sunspots. However, this is not an easy task because the Evershed flow is much stronger and may hide them in an efficient way, especially at low angular resolution. To minimize the problem, it is convenient to investigate the sunspot regions perpendicular to the line of symmetry, i.e., the line connecting the sunspot center with the disk center; there, the Doppler shifts induced by radial flows are zero, facilitating the detection of vertical motions. For an unambiguous identification of downflows using Doppler measurements, the spot should be as close to the disk center as possible, so that redshifts can reliably be associated with downflows and blueshifts with upflows.

Despite these problems, there have been some reports of small-scale convective motions in sunspot penumbrae. Sánchez Almeida et al. (2007) found a positive correlation between upward velocities and brightness from high-resolution spectroscopic measurements taken at the Swedish 1m Solar Telescope (SST). The observed correlation is reminiscent of normal convection, suggesting that a similar mechanism might be at work in the penumbra. Rimmele (2008) studied penumbral flows near the disk center using the Universal Birefringent Filter at the Dunn Solar Telescope. He de-

tected upflows in the dark core and downflows on either side of a penumbral filament, as expected from overturning convection. However, other filaments in the same filtergrams did not show downflows.

Using the Hinode satellite, Ichimoto et al. (2007) discovered an apparent twisting motion of brightness fluctuations in penumbral filaments located at $\pm 90^\circ$ from the symmetry line. The direction of the twist, as well as the associated Doppler signal (albeit at lower angular resolution), were consistent with transverse motions from the center of the filament to the edge facing the observer. Similar conclusions have been obtained by Bharti et al. (2010) from a larger sample of Hinode filtergrams. These authors measured twist velocities of more than 2.1 km s^{-1} in the portion of the filaments closer to the umbra and about 1 km s^{-1} at larger distances. Zakharov et al. (2008) reported the detection of Doppler signals compatible with horizontal overturning motions in a filament observed almost perpendicularly to the line of symmetry, 40° away from the disk center. Their measurements were taken with the SOUP magnetograph at the SST. The line-of-sight velocity of the horizontal motions was determined to be around 1 km s^{-1} from a Milne-Eddington inversion of the data. Unfortunately, the Fe I 630.25 nm line scans performed by Zakharov et al. required 123 s to be completed, meaning that any change in the flow field, solar scenery, or even seeing conditions during the scan could have affected the measurements. Velocities of 1 km s^{-1} extending over $0''.4$ seem within easy reach and should have been detected earlier.

By contrast, Franz & Schlichenmaier (2009) did not find indications of overturning downflows in Doppler velocity maps computed from spectropolarimetric observations taken with Hinode at a resolution of $0''.3$. Also the theoretical work of Borrero & Solanki (2010) suggests that small-scale overturning motions are not needed to explain the net circular polarization observed in the penumbra, since the much stronger Evered flow already accounts for it (see Borrero et al. 2007).

In view of these results, the existence of overturning convection cannot be considered as established. Thus, it is important to continue the search with measurements of the highest quality. Here we present an analysis of sunspot observations made with the Littrow spectrograph of the SST. The spot was located very close to the disk center, thus satisfying one of the requirements for good sensitivity to downward motions mentioned above. These observations reach a spatial resolution of about $0''.2$ and were used Bellot Rubio et al. (2005) to study the flow field of dark-cored penumbral filaments. To our knowledge, they are the highest spatial-resolution spectroscopic measurements of sunspot penumbrae ever obtained. The resolution is sufficient to distinguish the dark cores of penumbral filaments, which are only barely detectable in the seeing-free observations of the Hinode spectropolarimeter.

2. OBSERVATIONS AND DATA ANALYSIS

NOAA Active Region 10756 was observed with the Swedish 1 m Solar Telescope (Scharmer et al. 2003) on 2005 May 1. The best seeing conditions occurred at around 10:22 UT, when the heliocentric angle of the spot was 5° . Figure 1 shows a full disk MDI continuum image taken at 10:17 UT, while Figure 2 displays a context G-band continuum filtergram processed with the Multi-Frame Blind Deconvolution technique (van Noort et al. 2005). The resolution of the G-band continuum image approaches $0''.1$.

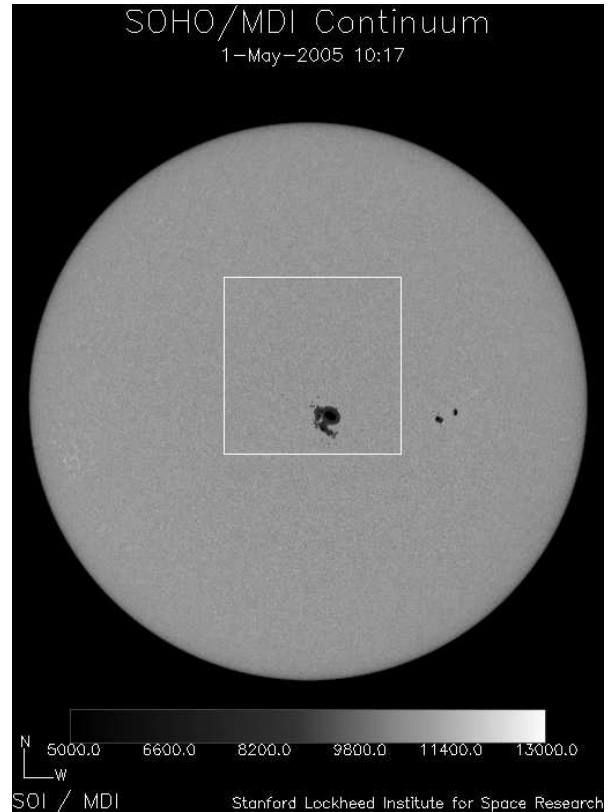


Figure 1. Full disk continuum image taken at 10:17 UT on 2005 May 1 by the Michelson Doppler Imager aboard SOHO. The spot closer to disk center is NOAA AR 10756, at coordinates $S6.9^\circ$ and $W4.3^\circ$. Courtesy Stanford Lockheed Institute for Solar Physics.

2.1. Spectroscopic observations

We used the TRI-Port Polarimetric Echelle-Littrow (TRIPPEL) spectrograph and the adaptive optics system of the SST to obtain line spectra at the highest angular resolution possible. TRIPPEL¹ has a grating of 79 grooves mm^{-1} , a blaze angle of 63.43° , and a theoretical resolving power of 240 000. Fe I 557.6 nm, Fe II 614.9 nm, and Fe I 709.0 nm were recorded simultaneously during the observations, but in this paper we consider only the 709.0 nm measurements because their short exposure times provided the best angular resolution.

Fe I 709.0 nm is a non-magnetic line suitable for Doppler shift measurements. Its narrow shape makes it very sensitive to line-of-sight velocities (Cabrera Solana et al. 2005). We performed spectroscopic observations of the region around 709 nm with a wavelength sampling of 1.046 pm, a pixel size of $0''.04$, and an exposure time of 200 ms. The spectra were recorded on a Kodak Megaplug 1.6i camera. The spectrograph slit had a width of $0''.11$ ($25 \mu\text{m}$) and covered a length of $37''.8$ (945 pixels). Simultaneously, slit-jaw images were taken through a 1 nm wide filter centered at 694 nm, also with exposure times of 200 ms.

The main advantage of slit spectrographs over tunable filters is that they record the full line profile at once, thus preserving spectral integrity. The disadvantage is that the solar image has to be stepped across the spectrograph slit to create

¹ See http://dubshen.astro.su.se/wiki/index.php/TRIPPEL_spectrograph

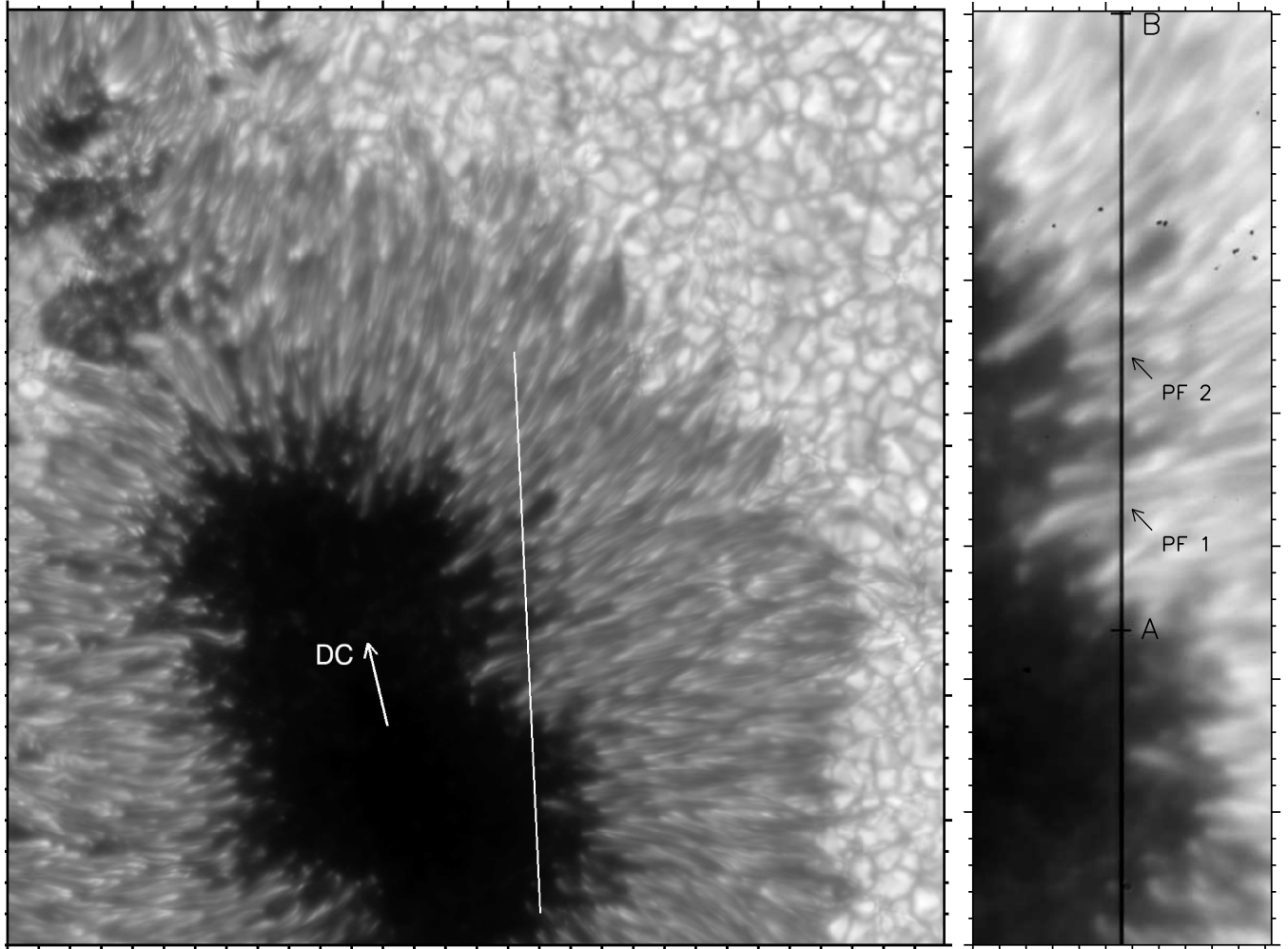


Figure 2. Left: G-band continuum image of AR 10756 obtained on 2005 May 1 at 10:22 UT through a 1.1 nm wide filter centered at 436.4 nm. The image has been reconstructed from five individual filtergrams of 20 ms exposure time. The arrow marks the direction to disk center (DC). The white line represents the spectrograph slit. It samples the umbra, the inner penumbra perpendicular to the symmetry line, and part of the center-side penumbra. Right: Slit-jaw image at 694 nm corresponding to the spectra discussed in this paper. The small dashes A and B indicate the portion of the slit shown in Figure 3. Two dark-cored penumbral filaments (PF 1 and PF 2) are clearly seen at the positions indicated by the arrows.

2D maps. We performed 20''-wide scans of the spot, but only a few slit positions attained a spatial resolution better than 0.''25. For this reason we concentrate on the best slit position, not on the entire map. As can be seen in Figure 2, the slit crossed the center-side penumbra and the region perpendicular to the line of symmetry near the umbra, providing a wide range of positions where overturning convection could occur.

The spectral images have been corrected for dark current, flatfield, and optical distortions (smile and keystone). The latter produce curvature of the spectral lines and a variation of the dispersion along the slit, respectively. More details can be found in Langangen et al. (2007).

2.2. Velocity measurements

We derive absolute velocities from the observed spectra as follows. First, we set up a relative wavelength scale using the dispersion obtained from the pixel separation between two lines with well-determined solar wavelengths in the corrected flatfield images. To calibrate this scale in absolute terms, it is necessary to fix the wavelength of one pixel in the spectrum. We use the telluric H₂O line at 709.4050 nm for that purpose.

The H₂O line is present in the same spectral region and is not affected by motions in the solar atmosphere, so it provides an excellent reference. Its central wavelength has been obtained from the Fourier Transform Spectrometer atlas of the quiet Sun by Brault & Neckel (1987) with a precision better than 50 m s⁻¹. For each height along the slit, we determine the position of the H₂O line core by means of a parabolic fit. The derived values show pixel-to-pixel fluctuations of 110 m s⁻¹ due to the weakness of the line, but we reduce them down to 40 m s⁻¹ applying a 12-pixel boxcar average along the slit. The final result is one position in each spectrum with a very precise wavelength (that of the H₂O line), i.e., an absolute wavelength scale.

The spectrally resolved profiles of Fe I 709.0 nm are used to derive Doppler shifts by means of line bisectors. We compute bisectors for intensity levels from 0% to 88%, where 0% represents the line core and 100% the continuum², through linear interpolation of the original wavelength samples. The bisec-

² We do not consider intensity levels higher than 88% to avoid the CN blend present in the very far red wing of the Fe I line (at 709.069 nm).

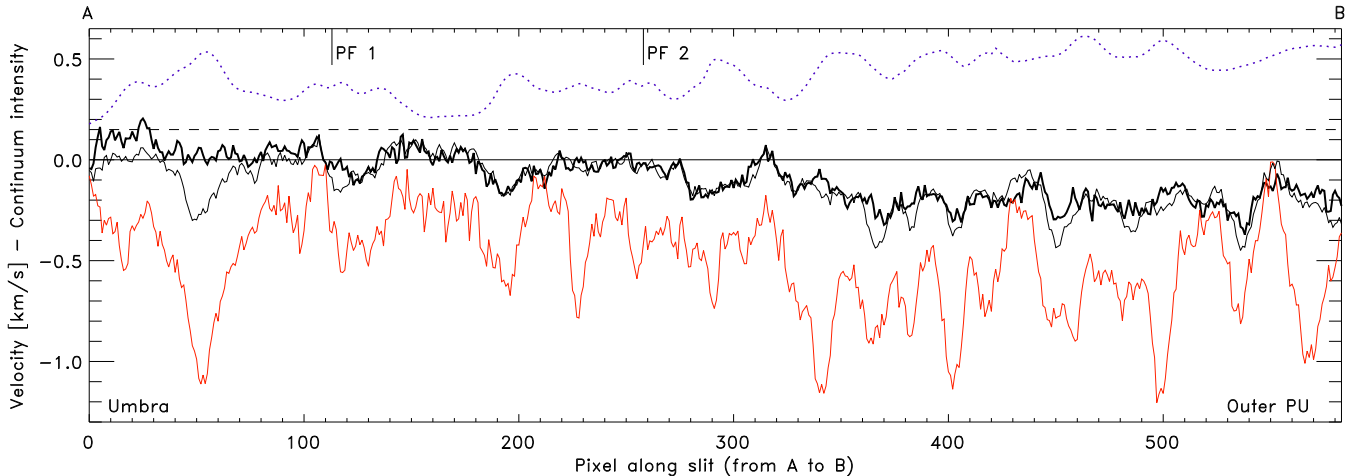


Figure 3. Absolute line-of-sight velocities derived from the line bisectors at different intensity levels: 0-8% (thick black line), 50-58% (thin black line), and 80-88% (red line). Positive velocities indicate redshifts. Since the spot was very near the disk center, they most likely correspond to downflows. The horizontal solid and dashed lines mark velocities of 0 and 150 m s^{-1} , respectively. The dotted blue line displays the continuum intensity along the slit, in a relative scale. The vertical lines labeled PF1 and PF2 in the upper abscissa mark the position of the two dark-cored penumbral filaments crossed by the slit (see Figure 2).

tor positions are converted into Doppler shifts by subtracting the laboratory wavelength of the Fe I line (709.03835 nm according to Nave et al. 1994), and then transformed into line-of-sight velocities.

Different intensity levels sample different layers of the atmosphere. Generally speaking, higher bisector intensities correspond to deeper layers. In the penumbral atmosphere of Bellot Rubio et al. (2006), the far line wing (as represented by intensities between 80% and 88%) is formed in the first 100 km above optical depth unity, i.e., the bisector Doppler shifts measured in this range reflect flow velocities from the very deep photosphere.

The bisector velocities still need to be corrected for gravitational redshift (636 m s^{-1}) and relative motions between the Sun and the observer. The former, computed as explained by Martínez Pillet et al. (1997), amount to $+316 \text{ m s}^{-1}$, of which -261 m s^{-1} correspond to the Earth’s rotation, $+436 \text{ m s}^{-1}$ to the Earth’s orbital motion, and $+141 \text{ m s}^{-1}$ to the solar rotation at the position of the spot (negative velocities are blueshifts).

Our *absolute* velocity calibration does not rely on the granulation or the umbra, and therefore it is not affected by uncertainties in the convective blueshift of the line or the presence of umbral flows. The main source of systematic errors comes from the laboratory wavelength of Fe I 709.0 nm, which has an uncertainty of about 100 m s^{-1} (Nave et al. 1994). Another source of systematic error is the central wavelength of the reference H_2O line (50 m s^{-1}). These errors add linearly, so the maximum systematic error of our calibration is 150 m s^{-1} . The effect of a systematic error is to shift all the velocities up or down as a whole. In contrast, the pixel-to-pixel “noise” of the velocity curves is due to random errors. We estimate the random error to be on the order of 110 m s^{-1} . This error comes from uncertainties in the position of the reference H_2O line (40 m s^{-1}) and uncertainties in the determination of the bisector position (about 100 m s^{-1}), added quadratically. All in all, our velocity measurements should be accurate to within $\pm 110 \text{ m s}^{-1}$, with systematic errors below 150 m s^{-1} .

3. RESULTS

Figure 3 shows the Doppler velocities observed along the slit, excluding the dark umbra where it is not possible to com-

pute reliable positions for the weak H_2O line. The outer part of the center-side penumbra is to the right. Displayed are line-core and line-wing velocities corresponding to the bisector shifts averaged between the 0% and 8% intensity levels (thick black line), between 50% and 58% (thin black line), and between 80% and 88% (red line). As mentioned before, higher intensity levels progressively sample deeper layers of the photosphere. For reference, the horizontal lines indicate velocities of 0 and 150 m s^{-1} (positive values represent redshifts). The continuum intensity is shown in the top part of the figure to help identify bright and dark structures (dotted blue line).

The first thing to note from Figure 3 is the tendency of all the velocities to increase toward more blueshifted values as the outer penumbra is approached, i.e., from left to right. This is due to two reasons: the strong enhancement of the magnitude of the Evershed flow with radial distance from the spot center (which compensates the increasing inclination of the flow), and the more favorable projection of the flow velocity to the line of sight toward the upper end of the spectrograph slit. Indeed, the angle between the penumbral filaments and the line of sight decreases from about 90° near the umbra to about 40° at the top of the slit; since the Evershed flow occurs along the filaments, the projection leads to stronger Doppler velocities. At a heliocentric angle of only 5° , however, the first effect is dominant.

We also note that the bisector velocities corresponding to intensity levels of 0%-8% and 50%-58% are very similar. This means that the lower half of the line show essentially vertical bisectors (i.e., no line asymmetries). By contrast, the velocities are substantially larger and to the blue in the far wings. Because of the larger velocities at high intensity levels, the bisectors are tilted to the blue near the continuum. Figure 4(a) displays a typical example: the strong tilt is caused by a “satellite” that starts to be visible in the far blue wing of the line. Also depicted in the figure are bisectors showing a more gradual (but strong) shift to the blue near the continuum, as well as cases of vertical bisectors with zero velocities and bisectors showing a tilt to the red. The latter, however, are not common in this part of the penumbra.

Deep in the atmosphere, as sampled by the bisectors near

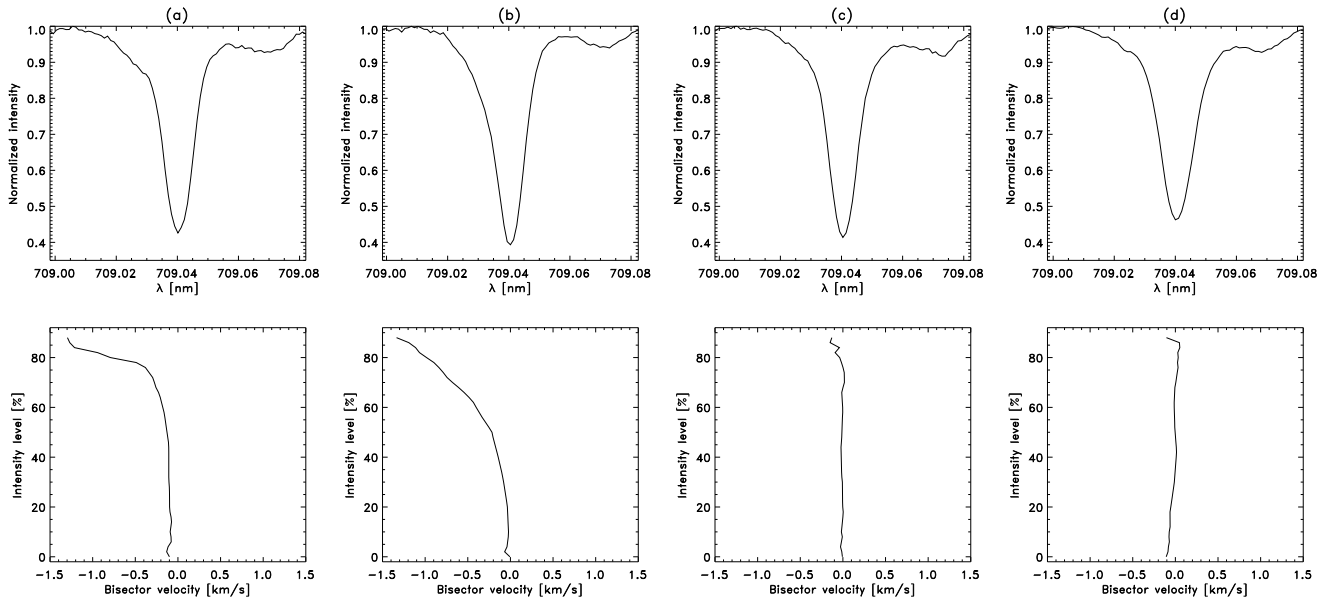


Figure 4. Examples of Fe I 709.0 nm line profiles (top) and bisectors (bottom) at different positions along the slit. (a) Vertical bisectors with a strong tilt to the blue near the continuum. (b) Strongly tilted bisectors showing larger blueshifts toward the continuum. (c) Vertical bisectors with zero velocities. (d) Bisectors tilted to the red toward the continuum. These examples correspond to pixel positions 338, 54, 209, and 552 in Figure 3, respectively.

the continuum, we always find blueshifts or zero velocities along the slit. The maximum blueshifts reach 1.2 km s^{-1} and tend to be cospatial with bright penumbral filaments, although we sometimes see a small displacement of the maximum velocity away from the observer, relative to the peak brightness position. In the dark regions outside of the filaments we also detect blueshifts for the most part. However, the velocities are strongly reduced. Sometimes they even drop to zero (e.g., Figure 4c). Although these instances are not common, this is the first time that zero velocities are observed in dark areas of the center-side penumbra. Earlier measurements at lower spatial resolution did not reveal them (e.g., Hirzberger & Kneer 2001; Rouppe van der Voort 2002; Bellot Rubio et al. 2006). The blueshifts depicted in Figure 3 may represent radial flows along inclined flux tubes. In that case, one would expect very small or no plasma motions in between the flow channels. However, this is not observed. The relative absence of zero velocities in our data may indicate that the tubes are still partly unresolved, or that there is some amount of stray light contamination. Another possibility is that the volume outside the flow channels is not completely at rest, as suggested by Stokes inversions (e.g., Bellot Rubio et al. 2004; Borrero et al. 2005) and net circular polarization measurements with Hinode (Ichimoto et al. 2008).

The line-core shifts (thick black curve in Figure 3) are much smaller than their line-wing counterparts. They do not exceed 200 m s^{-1} except in the middle center-side penumbra. Most of the positions along the slit show blueshifts. Redshifts do also occur, but with velocities of less than $100\text{-}150 \text{ m s}^{-1}$. These values are smaller than the systematic errors of our absolute velocity calibration. Apparently, the redshifts do not bear any relationship to the penumbral filaments: sometimes they occur on one side of the filament, sometimes on the other. The only exception is perhaps the structure located at pixel position 20, which shows relatively constant redshifts of about 100 m s^{-1} . This filament makes an angle of about 90° to the symmetry line.

It is also important to note that the dark-cored penumbral filaments crossed by the slit (PF 1 and PF 2 in Figure 3) do not exhibit blueshifts in the dark lanes and redshifts in the two lateral brightenings, contrary to what would be expected from a resolved overturning flow structure.

4. DISCUSSION

The observations analyzed in this paper are very favorable for the detection of downflows in the penumbra because they correspond to a sunspot located only 5° away from disk center. The contribution of horizontal flows to the observed Doppler signals is small, and redshifts/blueshifts can safely be associated with vertical downflows/upflows. Moreover, our observations provide full line profiles at the highest angular resolution achieved in this kind of measurements (better than $0''.25$), including a telluric line that we have employed to calibrate the velocity scale in absolute terms.

Despite the excellent quality of the data set, we do not detect downflows that could be associated with overturning convection in deep layers: near the continuum the measured velocities are always to the blue. Higher in the atmosphere, as sampled by the line core, we observe some regions that could harbor downflows, but with small velocities not exceeding 150 m s^{-1} . The fact that they are visible only in high layers suggests that they are not related to convective processes in the deep photosphere. They could be produced by downflows associated with the inverse Evershed flow, but also by penumbral oscillations or waves. In the absence of time series we cannot decide between the different scenarios.

Overall, our data suggest that downflows due to overturning convection are not larger than 150 m s^{-1} in the photospheric layers accessible to the observations, while the simulations predict values up to 1.5 km s^{-1} . The lack of a clear detection of overturning downflows may simply indicate that they do not exist. However, it is also possible that they have gone undetected if (a) they occur beneath $\tau = 1$; (b) they have velocities smaller than 150 m s^{-1} ; (c) they are concentrated in very

thin sheets not resolved by our observations; or (d) they fill only a small fraction of the formation region of the 709.0 nm line.

To examine possibility (c) we need spectroscopy at a resolution of 0.1 or better. Even with infinite spatial resolution, (d) may hamper the detection of the downflows if their vertical extent is much smaller than the width of the contribution functions of typical photospheric lines. In fact, the simulations show that the downflow lanes surrounding the penumbral filaments are not completely perpendicular to the solar surface, so that at some points they have a thickness of only 50-100 km in the vertical direction (e.g., Figure 9 of Rempel et al. 2009a). Such small structures may not be able to leave clear signatures in the emergent intensity profiles. Line synthesis calculations based on the simulation results are needed to clarify this aspect. If Fe I 709.0 nm does not provide sufficient height resolution, then the search for overturning downflows should be continued using lines with narrower contribution functions, like C I 538.03 nm. Another requirement to make progress is to increase the realism of the simulations. Current simulations reproduce many of the observed characteristics of the penumbra, but they predict downflows that we do not detect in spite of our excellent spatial, temporal, and spectral resolution. Thus, it is important to confirm that their results are not affected by too large values of the viscosity and magnetic diffusivity, by inadequate boundary conditions, or by too shallow computational boxes. Hopefully, the combination of these observational and numerical efforts will lead to a better understanding of the penumbra and the Evershed flow.

Financial support by the Spanish Ministerio de Ciencia e Innovación through project AYA2009-14105-C06-06 and by Junta de Andalucía through project P07-TEP-2687 is gratefully acknowledged. The Swedish 1 m Solar Telescope is operated by the Institute for Solar Physics of the Royal Swedish Academy of Sciences in the Spanish Observatorio del Roque de los Muchachos of the Instituto de Astrofísica de Canarias. This research has made use of NASA's Astrophysical Data System.

REFERENCES

- Bharti, L., Solanki, S. K., & Hirzberger, J. 2010, *ApJ*, in press, arXiv:1009.2919
- Bellot Rubio, L.R. 2010, in *Astrophysics and Space Science Proceedings, Magnetic Coupling between the Interior and the Atmosphere of the Sun*, ed. S. S. Hasan & R. J. Rutten (Berlin: Springer), 193
- Bellot Rubio, L. R., Balthasar, H., & Collados, M. 2004, *A&A*, 427, 319
- Bellot Rubio, L.R., Langhans, K., Schlichenmaier, R. 2005, *A&A*, 443, L7
- Bellot Rubio, L. R., Schlichenmaier, R., & Tritschler, A. 2006, *A&A*, 453, 1117
- Borrero, J. M. 2009, *Science in China G*, 52, 1670
- Borrero, J. M., Lagg, A., Solanki, S. K., & Collados, M. 2005, *A&A*, 436, 333
- Borrero, J. M., Bellot Rubio, L. R., Müller, D. A. N. 2007, *ApJ*, 666, L133
- Borrero, J. M., & Solanki, S. K. 2010, *ApJ*, 709, 349
- Brault, J., & Neckel, H. 1987, *Spectral Atlas of Solar Absolute Disk-averaged and Disk-center Intensity from 3290 to 12510 Å* (Hamburg: Hamb. Sternw.), <ftp://ftp.hs.uni-hamburg.de/pub/outgoing/FTS-Atlas>
- Cabrera Solana, D., Bellot Rubio, L. R., & del Toro Iniesta, J. C. 2005, *A&A*, 439, 687
- Degenhardt, D. 1989, *A&A*, 222, 297
- Franz, M., & Schlichenmaier, R. 2009, *A&A*, 508, 1453
- Heinemann, T., Nordlund, Å., Scharmer, G. B., & Spruit, H. C. 2007, *ApJ*, 669, 1390
- Hirzberger, J., & Kneer, F. 2001, *A&A*, 378, 1078
- Ichimoto, K., et al. 2007, *Science*, 318, 1597
- Ichimoto, K., et al. 2008, *A&A*, 481, L9
- Langangen, Ø., Carlsson, M., Rouppe van der Voort, L., & Stein, R. F. 2007, *ApJ*, 655, 615
- Nave, G., Johansson, S., Learner, R. C. M., Thorne, A. P., & Brault, J. W. 1994, *ApJS*, 94, 221
- Nordlund, Å., & Scharmer, G. B. 2010, in *Astrophysics and Space Science Proceedings, Magnetic Coupling between the Interior and the Atmosphere of the Sun*, ed. S. S. Hasan & R. J. Rutten (Berlin: Springer), 243
- Martínez Pillet, V., Lites, B. W., & Skumanich, A. 1997, *ApJ*, 474, 810
- Meyer, F., & Schmidt, H. U. 1968, *Zeitschrift Angewandte Mathematik und Mechanik*, 48, 218
- Montesinos, B., & Thomas, J. H. 1997, *Nature*, 390, 485
- Rempel, M., Schüssler, M., & Knölker, M. 2009a, *ApJ*, 691, 640
- Rempel, M., Schüssler, M., Cameron, R. H., & Knölker, M. 2009b, *Science*, 325, 171
- Rimmele, T. 2008, *ApJ*, 672, 684
- Rouppe van der Voort, L. H. M. 2002, *A&A*, 389, 1020
- Sánchez Almeida, J., Márquez, I., Bonet, J. A., & Domínguez Cerdeña, I. 2007, *ApJ*, 658, 1357
- Scharmer, G. B. 2009, *Space Science Reviews*, 144, 229
- Scharmer, G. B., Bjelksjo, K., Korhonen, T. K., Lindberg, B., & Petterson, B. 2003, *Proc. SPIE*, 4853, 341
- Scharmer, G. B., Nordlund, Å., & Heinemann, T. 2008, *ApJ*, 677, L149
- Schlichenmaier, R. 2002, *Astronomische Nachrichten*, 323, 303
- Schlichenmaier, R. 2009, *Space Science Reviews*, 144, 213
- Schlichenmaier, R., Jahn, K., & Schmidt, H. U. 1998, *A&A*, 337, 897
- van Noort, M., Rouppe van der Voort, L., Löfdahl, M. G. 2005, *Sol. Phys.*, 228, 191
- Zakharov, V., Hirzberger, J., Riethmüller, T. L., Solanki, S. K., & Kobel, P. 2008, *A&A*, 488, L17